Int. J. Heat Mass Transfer. Vol. 33, No. 4, pp. 641–648, 1990
Printed in Great Britain

0017–9310/90 $3.00 + 0.00
Pergamon Press plc

Heat transfer in supersonic coaxial reacting jets

S. I. BARANOVSKY, V. M. LEVIN, A. S. NADVORSKY and A. I. TURISHCHEV
S.Ordzhonikidze Aviation Institute, Moscow, 125871, U.S.S.R.

(*Received* 20 *March* 1986 *and in final form* 24 *November* 1988)

Abstract—The paper deals with the study of thermal and gas dynamics of coaxial supersonic turbulent reacting jets of hydrogen and air at a low initial oxidation temperature, the air being contaminated with combustion products of petrol B-70. The two-dimensional mathematical model involves the k–ε turbulence model, modified for supersonic compressibility, and a detailed kinetic mechanism of mixture combustion. The possibility is shown for the present authors' experiments to be correctly described within the framework of the theory developed. Different aspects of this kind of flow are studied allowing the construction of its general scheme.

1. INTRODUCTION

TODAY THE process of supersonic combustion is the sole means of effective energy conversion in a variety of technical apparatus. One of the most commonly used schemes [1] for the organization of combustion in a supersonic flow is a diffusional flare formed when a supersonic stream of a gaseous fuel (usually hydrogen) emerges into an accompanying stream of heated air [2]. In the majority of relevant works the cases were studied in which the static temperature of air considerably exceeded the spontaneous ignition temperature of hydrogen [2–4]. In these cases chemical reaction rates turned out to be rather high, the ignition delay time became exceedingly small and the entire process of combustion was controlled by turbulent mixing. In some instances, calculational methods based on the diffusional model of combustion allow one to satisfactorily represent the qualitative structure of the flow field [3, 5]. At the same time, more complex conditions are encountered in practice. First, the air temperature turns out to be close to the ignition limit, and this substantially increases the ignition delay time. Second, the process is greatly influenced by fluctuations of concentrations, and third, the facilities used to obtain experimental data involve different types of air preheaters that contaminate air with combustion products or with NO_x. The influence of all these factors has not as yet been studied adequately, and therefore the present complex study has been undertaken which includes experimental investigation of an isobaric supersonic jet of hydrogen in a coaxially supplied supersonic jet of a heated air and an attempt to create a mathematical model of such a jet which would take into account the effect of chemical kinetics, fluctuations of concentration and of the 'contamination' of the external air jet.

2. EXPERIMENTAL FACILITY

Experimental investigations were carried out on a rig (Fig. 1) which is an air combustion heater with a shaped supersonic nozzle the diameter of which at the exit is 70 mm and inside of which there is a central coaxially located body with a nozzle for co-current supply of gaseous hydrogen at the temperature $T_1 = 300$ K. The Mach number is $M_1 = 1.471$, the diameter of the central nozzle is 11.6 mm. The thickness of the inner nozzle edges is 0.2 mm. The oxidant flow parameters are: $M_2 = 2.33$, $T_2^* = 1800$ K. The heating is carried out by burning petrol B-70, with an additional supply of oxygen to restore its volumetric

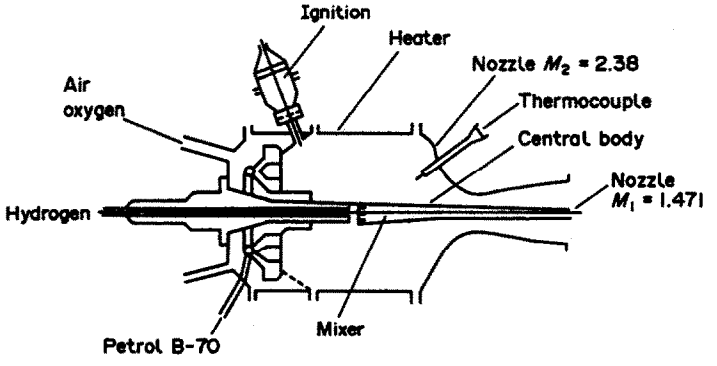

FIG. 1. Basic diagram of the set-up

NOMENCLATURE

C_i non-dimensional volumetric fraction of ith chemical component
f function of mixing layer geometry
g r.m.s. fluctuation of concentration
G_{air}, G_f, G_{O_2} mass flow rates of air, fuel and oxygen
h total enthalpy
K kinetic energy of turbulence
K_f, K_b constants of direct and reverse rates of chemical components
m_i mass fractions of chemical components
M_1, M_2 Mach numbers
Pr Prandtl number
r coordinate in cylindrical coordinate system
Sc Schmidt number
T_1, T_2 static temperature of internal and external flow
T_1^* stagnation temperature
u velocity component
v velocity component
$\bar{x}$ non-dimensional coordinate, abscissa.

Greek symbols
Γ_Φ coefficient in equation for Φ
η passive scalar
μ_{H_2O} molecular weight of water
μ_l, μ_t laminar and turbulent viscosity
ρ density
σ Prandtl–Schmidt effective numbers
Φ independent variable.

Subscripts
i,e internal and external boundaries of mixing layer
l laminar
t turbulent
1 internal flow
2 external flow.

concentration. The flow rates of the fuel and oxidants in the heater are: $G_f = 0.072096$ kg s^{-1}, $G_{air} = 1.724411$ kg s^{-1}, $G_{O_2} = 0.314208$ kg s^{-1}. Since flow velocities in the heater G_{air} are not high, the fuel burn-out is regarded to be complete and, using the equilibrium combustion model, the dimensionless mass concentrations of chemical components are determined to be equal to: $m_{O_2} = 0.2212$; $m_{H_2O} = 0.04396$; $m_{N_2} = 0.6277$; $m_{NO} = 0.2095 \times 10^{-5}$; $m_{CO_2} = 0.1071$. A selective chemical analysis for the content of O_2 and CO_2 confirmed the result of calculation. A chromatographic analysis also effects the absence of any compounds of carbon in air except for CO_2.

The static pressure in jets at the tip of the nozzles differed from the atmospheric one by no more than 3%. Special attention was payed to the possibility of obtaining a uniform stagnation pressure field. The maximum nonuniformity of the field at the nozzle exits does not exceed 5% (Fig. 2).

In all of the modes investigated the fuel self-ignited in a flow of oxidant. The oxidant flow velocity was found from the results of pressure measurements in the heater and at the nozzle tip with the thermodynamic properties of combustion products taken into account. The temperature in the heater was determined by means of a platinum–platinum–rhodium thermocouple.

The gasdynamic structure of the flow was investigated with the aid of unique small-size (the midsection is smaller than 1 mm) cooled total and static pressure detectors. The total pressure nozzle was also used for gas sampling. For a chemical analysis, an automated system of sampling was employed which

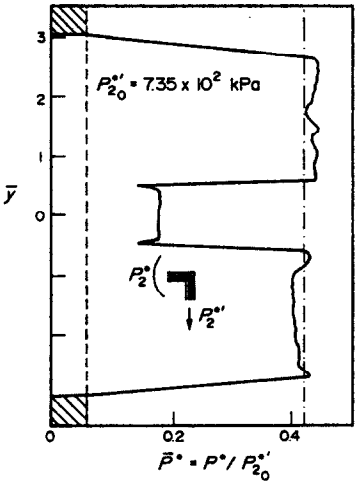

FIG. 2. Measured pressure stagnation field at the heater nozzle cut (oscilloscopic trace).

was coordinated with a positioning device. Still photographs were taken of the flare.

3. MATHEMATICAL MODEL OF THE FLOW

As is known, calculated supersonic gas streams can be described with the aid of the boundary layer approximation. In this case, the system of conservation equations reduces to the generalized equation of the form:

$$\rho u \frac{\partial \Phi}{\partial x} + \rho V \frac{\partial \Phi}{\partial r} = \frac{1}{r} \frac{\partial}{\partial r} \left[\Gamma_\Phi r \frac{\partial \Phi}{\partial r} \right] + S_\Phi \qquad (1)$$

with the following coefficients:

Φ	Γ_Φ	S_Φ	
u	$\mu_l+\mu_t$	0	(2)
h	$\frac{\mu_l}{Pr_l}+\frac{\mu_t}{Sc_t}$	$\frac{1}{r}\frac{\partial}{\partial r}\left\{r\mu_t\left[\left(1-\frac{1}{Pr_t}\right)u\frac{\partial u}{\partial r}+\left(\frac{1}{\sigma_k}-\frac{1}{Pr_t}\right)\frac{\partial K}{\partial r}\right]\right\}$	(3)
K	$\frac{\mu_l}{Pr_l}+\frac{\mu_t}{Pr_t}$	$\mu_t\left(\frac{\partial u}{\partial r}\right)^2-\rho\varepsilon$	(4)
ε	$\frac{\mu_l}{Pr_l}+\frac{\mu_t}{Pr_t}$	$C_{\varepsilon_1}\frac{\varepsilon}{K}\mu_t\left(\frac{\partial u}{\partial r}\right)^2-C_{\varepsilon_2}\frac{\varepsilon^2}{K}\rho$	(5)
m_i	$\frac{\mu_l}{Pr_l}+\frac{\mu_t}{Pr_t}$	$\sum_{j=1}^{S}(\nu''_{ij}-\nu'_{ij})\left[K_f^j\prod_{i=1}^{N}(m_i)^{\nu'_{ij}}-K_B^j\prod_{i=1}^{N}(m_i)^{\nu''_{ij}}\right.$	(6)
g_i	$\frac{\mu_l}{Pr_l}+\frac{\mu_t}{Pr_t}$	$C_{g_1}\mu_t\left(\frac{\partial m_i}{\partial r}\right)^2-C_{g_2}\left(\frac{\varepsilon}{K}\right)\rho g_i$	(7)

where u is the longitudinal velocity component, h the enthalpy, m_i the mass fractions of chemical elements, $g_i=(m_i-\bar{m}_i)^2$. Use is made of the Launder–Jones 'k–ε' two-parameter model of turbulence [6] which involves standard coefficients and into which the correction for 'compressibility' [7] is introduced

$$\mu_t = C_\mu \rho \frac{K^2}{\varepsilon} \tag{8}$$

where

$$C_\mu = \begin{cases} 0.09-0.04f & f\geqslant 0;\quad M<1 \\ 0.09-0.04f/M & f\geqslant 0;\quad M\geqslant 1 \\ 0.09-0.04/M & f<0;\quad M\geqslant 1 \end{cases} \tag{9}$$

M is the Mach number, and f the conventional function of mixture layer geometry [6].

Conventional pressure relations were employed

$$P=\rho RT/\mu_\Sigma. \tag{10}$$

The molecular viscosity of separate chemical components was determined from the Sutherland formula

$$\mu_t = BT^{3/2}/(S+T) \tag{11}$$

in which the coefficients B and S were derived by processing the data of ref. [8]. The viscosity of radicals was not taken into account.

The initial velocity profile corresponded to experimental data. For each of the three 'shear' layers, its 'effective' thickness $y_G=|y_2-y_1|$ was estimated

$$(u-u_i)/(u_e-u_i) = \begin{cases} 0.1 & \text{at} \quad y=y_1 \\ 0.9 & \text{at} \quad y=y_2 \end{cases}. \tag{12}$$

Then, using the Prandtl turbulence model *mlh* [6] and the fact that the kinetic energy of turbulence $K=|\overline{uv}|/0.3$, it is possible to obtain

$$K = y_G^2\left(\frac{\partial u}{\partial y}\right)^2\lambda^2/0.03. \tag{13}$$

Analogously

$$\varepsilon = K^{3/2}\lambda/(0.875y_G). \tag{14}$$

However, when $\partial u/\partial y\cong 0$, $K\cong 0$, $\varepsilon\cong 0$ the quantity μ_t in equation (8) also becomes (when being calculated on a computer) indeterminate. There can arise 'disagreement' between k and ε which leads rapidly to a non-physical result. This situation can be avoided by using a 'rough' estimate

$$K_{\min} = Au^2. \tag{15}$$

It is sufficient to select the constant A in such a way that $\mu_t \ll \mu_l$ when $\partial u/\partial y\approx 0$. The characteristic value $A=4\times 10^{-4}$. Finally

$$K=\max\{K, K_{\min}\}. \tag{16}$$

An estimate analogous to equation (15) was also employed when prescribing initial conditions for g_i

$$g_{\min} = \text{const}\cdot u^2. \tag{17}$$

There are no singularities in the assignment of boundary conditions—the symmetry conditions were assigned on the flow axis and the conditions of a non-perturbed flow on the outer surface.

The 'rigorous' equation (6) was solved by the Rosenbrock–Wenner technique of the fourth order with a variable step [9], the rest of the equations of the system were solved by the Patankar–Spalding technique with slight modifications. The 'splitting' principle was employed. The algorithm of the solution is described in ref. [9].

Two combustion models were used for calculation. The first model included the determining equilibrium reactions between the elements C, H, O, and N. In this case, concentration fluctuations were taken into account within the framework of the method of the probability density function (PDF) of the conservative scalar quantity (CSQ). As a CSQ, the mass fraction Z_H and Z_O will be introduced

$$Z_H = m_H + m_{H_2} + \left(\frac{\mu_{H_2}}{\mu_{H_2O}}\right)^* m_{H_2O} + \cdots \quad (18)$$

where μ_i/μ_j is the number of grams of the ith element per gram of the jth element. It is conceivable that, assuming identical diffusion coefficients for Z_H, it is possible to write down the mass conservation equation with a zero source term. During the mixing of two homogeneous flows the mass fractions of the elements reduce to the following normalized form:

$$\eta_1 = (Z_H - Z_{H,1})/(Z_{H,2} - Z_{H,1}) \quad (19)$$

in the first stream $\eta_1 = 0$ and in the second stream $\eta = 1$, i.e. the boundary conditions are identical for all Z_i's. Then equation (6) will also be valid for η_1, and with Z_i being known, all m_i's are recovered from linear relations. In the case of three streams this seems to be incorrect; it is necessary to introduce two coefficients of a mixture: η_1 and η_2. Note also that equation (19) holds only in the case when there is no transfer of m_i through the surfaces that bound the mixing. It turned out to be convenient in this work to solve equation (6) for Z_H, Z_O, Z_N and then to normalize them in such a way that $0 \leqslant \eta_i \leqslant 1$.

It is shown in ref. [10] that the flow field depends little on the form of the PDF used so long as the form of the dependence is 'physical' enough and correctly describes the 'nonmixedness'. Gaussian and truncated Gaussian distributions are widely used, but they lack explicit functions for the mean value and variance, and they are determined numerically by the iterative solution of a non-linear equation at each computational point. The truncated Gaussian distribution is physically incorrect [11]. Therefore, for the PDF in the present work the β-distribution was selected

$$P(\eta) = \eta^{\alpha-1}(1-\eta)^{\beta-1} \Big/ \int_0^1 d\eta\, \eta^{\alpha-1}(1-\eta)^{\beta-1},$$

$$0 \leqslant \eta \leqslant 1 \quad (20)$$

where α and β are determined explicitly

$$\alpha = \bar{\eta}\left(\frac{\bar{\eta}(1-\bar{\eta})}{(\eta-\bar{\eta})^2} - 1\right) \quad (21)$$

$$\beta = (1-\bar{\eta})\left(\frac{\bar{\eta}(1-\bar{\eta})}{(\eta-\bar{\eta})^2} - 1\right). \quad (22)$$

A satisfactory agreement between the β-function and the actual PDF is shown in ref. [12].

The second model of combustion (non-equilibrium) (Table 1) was developed by selecting the determining reactions in an H_2–O_2 mixture near the second and third limits of ignition on the basis of the criteria of ref. [13]. The specific features of this model are the capability to localize the II–IV ignition limits, a satisfactory description of the ignition delay time (IDT) and of the time of reaction. The model additionally involves reactions with NO and NO_2 [14] to take into account their effect on the IDT at low temperatures. The conversion of CO into CO_2 is represented by several stages [15].

In order that the concentration fluctuations could be taken into account, the simplest model of 'nonmixedness' [16] was employed according to which the corrections for the reaction rates K_{fi} and K_{bi} were introduced

$$\tilde{K}_{fi} = K_{fi}(1-\tilde{U}_{fi}); \quad \tilde{K}_{bi} = K_{bi}(1-\tilde{U}_{bi}) \quad (23)$$

where

$$\tilde{U}_{fi} = \tilde{U}_{fi}\left(\frac{g_i}{m_i}\right); \quad \tilde{U}_{bi} = \tilde{U}_{bi}\left(\frac{g_i}{m_i}\right). \quad (24)$$

4. RESULTS OF INVESTIGATION

Figure 3 shows distributions of the main parameters measured on the symmetry axis. Here $\bar{x} = x/d_1$, where d_1 is the diameter of the inner nozzle. The results of measurements indicate that the boundary of the initial section of the central jet comes in contact with the axis at $\bar{x} \cong 10$ when fuel and oxidant jets interact. Over this initial section the flow stagnation pressure preserves its constant value. Here, the dimensionless volumetric concentration of hydrogen $\bar{C}_{H_2}$ (in a dry sample) is constant and equal to 1. The end of the initial section can be identified by the appearance of nitrogen and of a small amount of O_2 on the jet axis at $\bar{x} = 10$–30 as a result of the diffusion of these components from the heated air stream. The presence of oxygen on the flow axis is attributed to the delay of ignition, to the absence of chemical interaction between a low-temperature hydrogen and a cooled wall layer of oxidant near the outer surface of the central body nozzle.

A characteristic bend can be noted in the plot of fuel concentration along the flow axis. The concentration drops sharply before the bend (by about 20%) due to the mixing with oxidant from the heater, whereas its further decrease is associated with the addition of the mass of air from stagnant surroundings. This is confirmed by an analogous behaviour of nitrogen concentration on the flow axis.

It is of interest to compare the appearance of oxygen on the axis with the visible flare boundary obtained by processing the photographs of the jet. The appearance of the glow is observed at $\bar{x} \cong 12.5$, i.e. at the

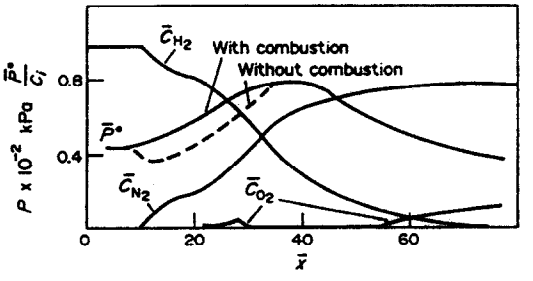

FIG. 3. Measured parameters on the flow axis

Table 1

No.	Reaction	Kj A	Kj α	Kj n	Kj β	K–j A	K–j α	K–j n	K–j β
1	$H_2+O_2=2OH$	1.475	13	—	19250	4.6	11	—	10230
2	$OH+H_2=H_2O+H$	1.144	9	1.3	1825	4.975	9	1.3	9355
3	$H+O_2=OH+O$	1.445	14	—	8250	1.165	13	—	280
4	$O+H_2=OH+H$	1.807	10	1	4480	7.994	9	1	3440
5	$2H+M=H_2+M$	1.088	18	−1	—	4.754	18	−1	52650
6	$H+OH+M=H_2O+M$	3.626	22	−2	—	6.766	23	−2	60180
7	$2OH+M=H_2O_2+M$	8.75	14	—	2832.5	1.2	17	—	2285.0
8	$H+O_2+M=H_2O+M$	7.253	15	—	−500	1.021	16	—	22960
9	$HO_2+H_2=H_2O_2+H$	7.25	11	—	9900	1.55	12	—	2000
10	$HO_2+H_2=H_2O+OH$	6.022	11	—	9400	2.737	11	—	37110
11	$HO_2+H_2O=H_2O_2+OH$	2.5	13	—	16250	1.15	13	—	0885
12	$2HO_2=H_2O_2+O_2$	3	12	—	—	1.25	11	0.5	20600
13	$H+HO_2=2OH$	2.409	14	—	950	2.590	13	—	21130
14	$H+HO_2=H_2O+O$	1.4	13	—	1045	0.55	13	—	29000
15	$H+HO_2=H_2+O_2$	2.409	13	—	350	7.299	13	—	29550
16	$O+HO_2=OH+O_2$	4.818	13	—	500	6.423	13	—	28660
17	$H+H_2O_2=H_2O+OH$	1	15	—	5350	1.15	14	—	39850
18	$OH+M=O+H+M$	6.843	18	−1	51610	3.626	18	−1	—
19	$HO_2+OH=H_2O+O_2$	3.011	13	—	—	3.962	14	—	36730
	$H_2/O_2/N_2$ (Zeldovich'es extended mechanism)								
20	$O+N_2=N+O$	7.6	13	—	38000	1.6	13	—	—
21	$H+NO=N+OH$	2	14	—	23650	1.0	14	—	—
22	$O+NO=N+O_2$	1.5	9	1	19500	6.4	9	1	3150
	$H_2/O_2/NO_x$								
23	$NO+OH=H+NO_2$	2.0	11	0.5	15500	3.5	14	—	740
24	$NO+O_2=O+NO_2$	1.0	12	—	22800	1.0	13	—	302
25	$NO_2+H_2=H+HNO_2$	2.4	13	—	14500	5.0	11	0.5	1500
26	$NO_2+OH=NO+HO_2$	1.0	11	0.5	6000	3.0	12	0.5	1200
27	$HNO_2+M=NO+OH+M$	5.0	17	−1	25000	8.0	15	—	−1000
28	$NO_2+M=NO+O+M$	1.1	16	—	32712	1.1	15	—	−941
	$H_2/O_2/CO_x$								
29	$CO+OH=CO_2+H$	1.686	7	1.3	−330	1.756	9	1.3	51610
30	$CO+HO_2=CO_2+OH$	1.506	14	—	11900	1.673	15	—	42950
31	$O+CO+M=CO_2+M$	2.539	15	0	2200	4.959	17	0	64670
32	$O+CO_2=O_2+CO$	2.107	13	0	26890	2.529	12	0	24000

end of the initial section. Two zones of increased luminosity can be identified: $\bar{x}=20$–25 and 35–40. The stretch $\bar{x}=20$–25 corresponds to the enhancement of combustion provided by the influx of pure air from the outside. Over the stretch 35–40, reaction proceeds within the entire mixing layer, including the symmetry axes, as indicated by the disappearance of oxygen in both experimental data and results predicted by the non-equilibrium combustion model. This is also responsible for a sharp drop of the total pressure on the flow axis. After $\bar{x}\cong 50$, again the presence of oxygen can be noted because the reaction slows down due to a great concentration of combustion products and a small amount of hydrogen which had not yet reacted.

A slight decrease of the static pressure along the jet axis is observed the fluctuational variation of which is ascribed to the wave structure generated by the weak non-isobaricity of flow on the nozzle tips and to heat generation in the mixing layer of supersonic streams having substantially different densities.

Using the fuel and oxygen concentrations at three sections as given in Figs. 4 and 5, it is possible to estimate the position of the stoichiometric surface during combustion. The sections are selected in which oxygen is present in the entire volume of the flare.

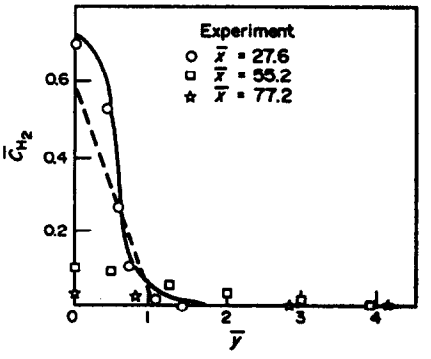

FIG. 4. Variation of the volumetric concentration of hydrogen in the cross sections of reacting jets. Prediction: $\bar{x}=27.6$. Dashed line, equilibrium model of combustion. Solid line, non-equilibrium combustion model.

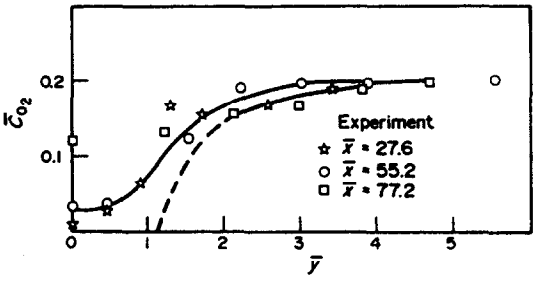

FIG. 5. Variation of the volumetric concentration of oxygen in cross-sections of reacting jets. Solid line, kinetics; dashed line, equilibrium combustion model. Prediction: $\bar{x} = 27.6$.

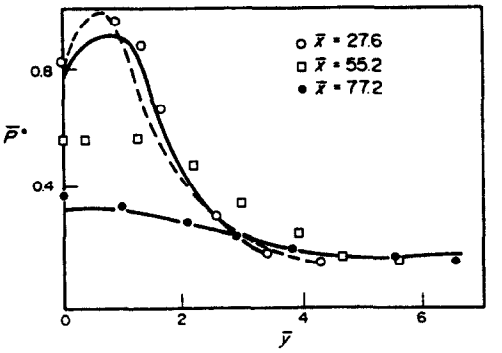

FIG. 6. Total pressure distribution in three sections. Prediction: $\bar{x} = 27.6$. Dashed line, equilibrium combustion model; solid line, kinetics; $\bar{x} = 77$, dashed line, non-equilibrium combustion model.

The equalization of concentration profiles and the penetration of hydrogen to the flow periphery is caused by the downstream build-up of the mixing layer and also by the interdiffusion of reagents. Here $\bar{C}_i$ are the dimensionless volumetric concentrations in a dry sample. The verification of the combustion models at the characteristic point $\bar{x} = 27.6$ shows that the equilibrium model does not allow calculation of a detailed gasdynamic and kinetic structure. In particular, the assumption of the infinite reaction rates leads to the impossibility of the existence of hydrogen and oxygen at one flow point, therefore the decay of H_2 concentration on the symmetry axis is strongly intensified, whereas heat generation turns to be much in excess of the actual one (Fig. 7). The kinetic model fundamentally correctly represents the occurring chemical phenomena, but tend to overshoot the content of O_2. This is probably due to a small non-isobaricity present in the experiment.

At the same time, the simple equilibrium combustion model, which requires several times less computer time, may be used to estimate more 'conservative' parameters, for example, stagnation pressure (Fig. 6).

Also noteworthy is another interesting phenomenon which was first observed in the first combustion model. The CO_2, which is present in a heated air, acts as an additional oxidant of hydrogen, with the stoichiometric point for c lying lower (in sections) than that for oxygen. By combining several stages, it is possible to obtain the reaction

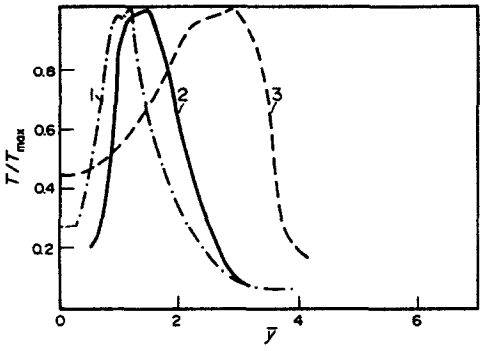

FIG. 7. Predicted distribution of the static temperature in two sections. $\bar{x} = 27.6$: dashed-dotted line (1), equilibrium combustion model; solid line, kinetics (2). $\bar{x} = 77.2$, dashed line, kinetics (3).

$CO_2 + H_2 = CO + H_2O$ which explains this process. An analogous phenomenon is also observed in the non-equilibrium combustion model, but here it is much less pronounced. The presence of two temperature peaks (Fig. 7) is due to the chemical interaction of hydrogen with carbon dioxide.

The flow model (Fig. 8) based on the above-given analysis makes it possible to explain the mechanism of interaction of supersonic coaxial streams in the presence of a substantial delay of ignition and preheated air contamination.

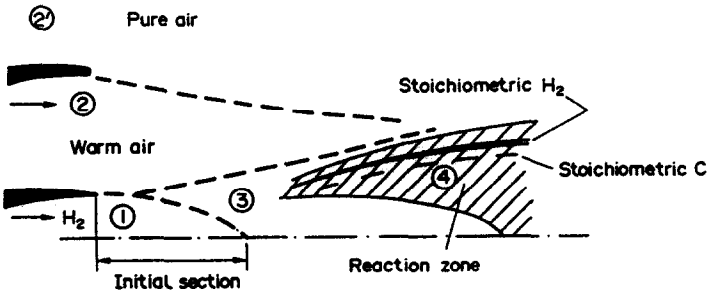

FIG. 8. Flow model.

The presence of two streams: cold hydrogen (1) and slightly heated contaminated air (2) that escape into the atmosphere air, leads to the formation of the zone of partially stirred mixture (3) due to which the fuel flow displays the presence of an oxidant which diffused from the outside. Moreover, they do not react until zone (3) becomes hotter than the overlying reaction zone (4).

Note that combustion is initiated near the edge of the inner nozzle where there are the best conditions, for mixing and ignition. Should the temperature of the oxidant be raised and thus the ITD be sharply reduced, zone (3) may not appear, and a conventional diffusional flare will be realized. Another important feature of the flow studied is the presence of two combustion surfaces due to contamination of the oxidant used.

It seems that the effects discovered in the present work should also be taken into account when constructing more complex mathematical models for combustion of supersonic turbulent coaxial jets that include the nonisobaricity, effect of shock waves, etc.

Acknowledgement—The authors are grateful to Professor G. N. Abramovich for a continuous interest in the work and valuable recommendations.

REFERENCES

1. V. K. Bayev, V. I. Golovichyov, P. K. Tretiyakov, A. F. Garanin, V. A. Konstantinovskiy and V. A. Yasakov, *Combustion in Supersonic Flow*. Izd. Nauka, Novosibirsk (1984).
2. L. S. Cohen and R. N. Guile, Investigation of mixing and combustion of turbulent compressible free jets, NASA CR-1473 (1969).
3. G. N. Abramovich, S. I. Baranovsky, V. M. Levin and A. S. Nadvorsky, Investigation of supersonic combustion. *Proc. 8th Int. Colloquium on Gas Dynamics of Explosions and Reactive Systems*. Izd. ITMO AN BSSR, Minsk (1981).
4. H. L. Beach, Jr., A study of reacting free and ducted hydrogen/air jets, NASA TMX 72678 (1972).
5. E. A. Meshcheryakov and V. A. Sabelnikov, A semi-empirical model and calculation of the intermittancy coefficient in turbulent jet flows, *Fiz. Gor. Vzryva* **20**(4), 45–52 (1984).
6. B. E. Launder, A. Morse, W. Rodi and D. B. Spalding, Prediction of free shear flows—a comparison of six turbulence models, NASA SP-321 (1973).
7. S. I. Baranovsky, A. S. Nadvorsky and T. F. Savina, Allowance for compressibility on supersonic submerged jets, *Izv. VUZov, Aviats, Tekhnika* No. 1, 11–15 (1986).
8. V. A. Golubev, *Viscosity of Gases and Gas Mixtures*. Fizmatgiz, Baku (1959).
9. V. N. Lutsenko, A. S. Nadvorsky and D. D. Romashkova, A technique for taking into account chemical non-equilibrium state for a numerical analysis of mixing and combustion of turbulent jets. In *The Theory of Aviation Engines*, pp. 92–101. Izd. Nauka, Moscow (1982).
10. J. H. Kent and R. W. Bilger, Turbulent diffusion flames, 16th Int. Symp. on Combustion, The Combustion Institute, Pittsburg, Pennsylvania (1977).
11. W. W. Colman (Editor), *Prediction Methods for Turbulent Flows* (in Russian). Izd. Mir, Moscow (1983).
12. M. Slack and A. Grillo, Investigation of hydrogen–air ignition sensitized by nitric oxide and by nitrogen dioxide, NASA CR 2876 (1977).
13. V. I. Dimitrov, *Simple Kinetics*. Izd. Nauka, Novosibirsk (1982).
14. B. P. Rhodes, A probability distribution function for turbulent flows. In *Turbulent Mixing in Nonreactive and Reactive Flows*, pp. 235–242. Plenum Press, New York (1974).
15. N. A. Chigir (Editor), *Formation and Decomposition of Contaminating Substances in a Flame*. Izd. Mashinostroyeniye, Moscow (1981).
16. E. Spiegler, M. Wolfshtein and Y. Manheimer-Timnat, A model of unmixedness for turbulent reactive flows, *Acta Astronautika* **3**, 265–280 (1976).

TRANSFERT THERMIQUE DANS DES JETS SUPERSONIQUES COAXIAUX EN REACTION

Résumé—On étudie la dynamique thermique et du gaz de jets supersoniques, coaxiaux, en réaction, d'hydrogène et d'air à faible température initiale d'oxydation, l'air étant contaminé par la combustion de produits pétroliers B-70. Le modèle mathématique bidimensionnel est du type k–ε, modifié pour tenir compte de la compressibilité supersonique et du mécanisme détaillé de la cinétique de combustion du mélange. On constate la possibilité de décrire correctement les expériences des auteurs. Différents aspects de ce type d'écoulement sont étudiés pour permettre la construction de son schéma général.

WÄRMEÜBERTRAGUNG IN REAGIERENDEN KOAXIALEN ÜBERSCHALLFREISTRAHLEN

Zusammenfassung—Die Thermo- und Gasdynamik eines reagierenden turbulenten koaxialen Wasserstoff/Luft-Überschallfreistrahls wird bei niedriger Zündtemperatur untersucht. Die Luft ist mit Verbrennungsprodukten von Benzin B-70 verunreinigt. Das zweidimensionale mathematische Modell beinhaltet ein für Überschall auf Kompressibilität erweitertes k–ε Turbulenzmodell und einen detaillierten reaktionskinetischen Mechanismus zur Gemischverbrennung. Es wird gezeigt, daß die Experimente des Autors im Rahmen der entwickelten Theorie richtig beschrieben werden. Verschiedene Gesichtspunkte dieser Strömungsart sind untersucht worden, was die Konstruktion eines allgemeinen Schemas erlaubt.

ТЕПЛООБМЕН В СВЕРХЗВУКОВЫХ КОАКСИАЛЬНЫХ РЕАГИРУЮЩИХ СТРУЯХ

Аннотация—Исследуется термо-газодинамика коаксиальных сверхзвуковых турбулентных реагирующих струй водорода и воздуха при низкой начальной температуре окисления, загрязненного продуктами сгорания бензина Б-70. Используемая двумерная математическая модель течения включает модифицированную на сверхзвуковую сжимаемость модель турбулентности k–ε, детальный кинетический механизм горения смеси. Показана возможность корректного описания собственных экспериментов авторов в рамках разработанной теории. Изучены различные особенности подобного течения, что позволило построить его общую схему.